Nuclear Instruments and Methods in Physics Research A 831 (2016) 24–28

Contents lists available at ScienceDirect

Nuclear Instruments and Methods in Physics Research A

journal homepage: www.elsevier.com/locate/nima

Recent technological developments on LGAD and iLGAD detectors for tracking and timing applications

G. Pellegrini [a,*], M. Baselga [a], M. Carulla [a], V. Fadeyev [b], P. Fernández-Martínez [a], M. Fernández García [d], D. Flores [a], Z. Galloway [b], C. Gallrapp [c], S. Hidalgo [a], Z. Liang [b], A. Merlos [a], M. Moll [c], D. Quirion [a], H. Sadrozinski [b], M. Stricker [c], I. Vila [d]

[a] Centro Nacional de Microelectrónica, IMB-CNM-CSIC, Barcelona, Spain
[b] Santa Cruz Institute of Particle Physics SCIPP, Santa Cruz, CA, USA
[c] CERN, Geneva, Switzerland
[d] Instituto de Física de Cantabria IFCA-CSIC-UC, Santander, Spain

ARTICLE INFO

Article history:
Received 19 November 2015
Received in revised form
25 April 2016
Accepted 17 May 2016
Available online 17 May 2016

Keywords:
Silicon detectors
Avalanche multiplication
Timing detectors
Tracking detectors

ABSTRACT

This paper reports the latest technological development on the Low Gain Avalanche Detector (LGAD) and introduces a new architecture of these detectors called inverse-LGAD (iLGAD). Both approaches are based on the standard Avalanche Photo Diodes (APD) concept, commonly used in optical and X-ray detection applications, including an internal multiplication of the charge generated by radiation. The multiplication is inherent to the basic n^{++}–p^{+}–p structure, where the doping profile of the p^{+} layer is optimized to achieve high field and high impact ionization at the junction.

The LGAD structures are optimized for applications such as tracking or timing detectors for high energy physics experiments or medical applications where time resolution lower than 30 ps is required. Detailed TCAD device simulations together with the electrical and charge collection measurements are presented through this work.

1. Introduction

All avalanche diode detectors [1] have a region with a high electrical field leading to multiplication of signal charges (electron and/or holes) flowing through this region. The gain mechanism is achieved within the semiconductor material by raising the electric field as high as necessary to enable the drifting electrons to create secondary ionization during the collection process. Normally, the junction consists of a thin and highly doped n-type layer on top of a moderately doped p-layer in which the multiplication (of electrons) takes place. A high resistivity p-type silicon substrate is typically used to produce detectors with a bulk that can be fully depleted.

Compared to standard APD detectors, LGAD (Low Gain Avalanche Detectors) and iLGAD (inverse LGAD) structures exhibit moderate gain values. This is mandatory to obtain fine segmentation pitches in the fabrication of microstrip and pixel detectors, free from the limitations commonly found in avalanche detectors [2]. In addition, a moderate multiplication allows the fabrication of thinner sensors, with an output signal amplitude that is as large as that from thicker sensors without internal gain. The design of LGAD and iLGAD structures exploits the charge multiplication effect to obtain a silicon detector that can simultaneously measure precisely the position and time of arrival of incident particles.

The process technology of LGAD detectors has already been introduced in the past [3] as well as radiation hardness studies [4]. Several wafers were fabricated with a highly doped p-type layer, implanted under the n^{+} shallow diffusion to reach the electric field strength [5] which provides the required gain. The structure is similar to the one of the Avalanche Photo Diodes but optimized for operation in the linear gain region. Breakdown above 1000 V can be targeted provided that the electrode isolation technique is properly designed for segmented sensors [6].

This report is describing the operation mode and performance of LGAD and iLGAD sensors. The internal gain in silicon sensors and its uniformity in segmented detectors are discussed. A new approach to the charge collection is also analyzed for the iLGAD structures where the segmentation is implemented at the ohmic contact (p^{+} diffusion at the back side of the LGAD). This ensures a uniform multiplication at the n^{+}p junction side. *I*(V) and *C*(V) performances and charge collection data obtained from α and laser measurements to get an estimation of the gain, are included. Finally, preliminary Technology Computer Aided Design (TCAD) numerical device simulation results of iLGAD detectors are reported.

* Corresponding author.

http://dx.doi.org/10.1016/j.nima.2016.05.066

2. Low gain avalanche detectors (LGAD)

Pad LGAD detectors have been fabricated and extensively measured. Three different designs were considered for the edge termination, based on the location of a deep n-type diffusion called Junction Termination Extension (JTE) [7]. All the detectors designs include a shallow n-type collector ring between the edge of the main junction and the device periphery allowing collecting the undesired leakage current generated at the periphery region. Design 1 includes JTE diffusion both in the main junction and the collector ring while for Design 2 the JTE is only placed at the collector ring. Finally, Design 3 does not include the JTE diffusion but only the shallow n+ implant. A detailed study of the termination structures used for the LGAD detectors was already published in [6].

LGAD detectors with the described edge termination designs were fabricated at the Instituto de Microelectrónica de Barcelona – Centro Nacional de Microelectrónica (IMB–CNM) Clean Room on 300 μm substrates. The last processed wafers have been measured to check the electrical performances, the charge collection capability and the yield. The *I*(V) curves plotted in Fig. 1 correspond to different detectors with edge termination according to design 1, the one with the highest voltage capability, and the optimum implantation dose of the p-well to obtain a gain of 10. These results suggest that the leakage current for LGAD devices with an area of 3×3 mm² is of the order of 10 to 30 nA for a supply voltage above 500 V. The yield, defined by devices with leakage current below 30 nA at 500 V is 76%. The yield is reduced to 72,5% at 1000 V (also devices with leakage current below 30 nA). Each wafer included 87 LGAD detectors. The $1/C^2$ (V) curves plotted in Fig. 2 show the different depletion spread in the pad LGAD detectors when compared with the PiN detectors fabricated within the same process technology suppressing the p-well implantation step. From the LGAD curve of Fig. 2, it can be inferred the reverse voltage at which the p-well becomes completely depleted (30 V) with the subsequent decrease of the capacitance value until the full depletion of the substrate at 80 V.

LGAD samples were characterized at IMB–CNM, Santa Cruz Institute of Particle Physics (SCIPP) and CERN. The gain of different samples with P-well implantation dose is shown in Fig. 3, where a relatively good linearity in the typical operating voltages (200–800 V) can be observed. The gain in this voltage range varies from 4.1–6.6. Measurements using the TCT technique with 1060 nm infrared laser and backside illumination, [8], revealed that a high uniformity of the electric field in the detection region is achieved.

Pad LGAD detectors can only provide a signal proportional to the energy deposited by the incident particle. Strip LGAD detectors provide combined information on energy deposited and position of the incident particle and are essential for high accuracy tracking applications. LGAD detectors with strip electrode pattern were also fabricated within the same wafer batch. The geometrical parameters of the strips are: total area 1 cm², pitch of 80 μm, a multiplication implant width of 20 μm and a junction implant width of 32 μm. Preliminary results show multiplication at the central part of each strip, as shown in Fig. 4, where the charge collected scanning three LGAD strips with a 661 nm red laser [8] from the front side is plotted for different reverse bias values. The charge is collected along a line perpendicular to the strips length. The top surface of the strips illuminated by the laser is not covered with aluminum. At a reverse bias of 50 V (Fig. 4 left) the substrate is not yet depleted and no multiplication is present in the structure. On the contrary, when the reverse bias is increased to 150 V (Fig. 4 right) the substrate is fully depleted and the multiplication is already active at the central part of each strip. Using the signal amplitude of 20 mV, obtained with a reference PiN diode (no multiplication), the experimental gain value for the strip sensors

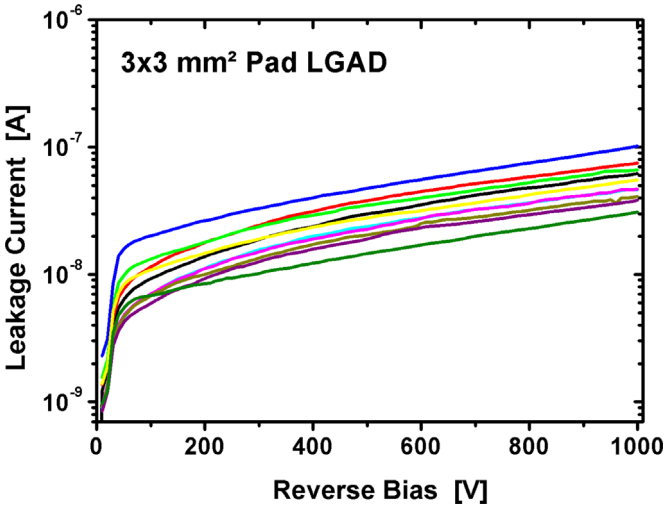

Fig. 1. *I*(V) curves of 300 μm pad LGAD detectors with edge termination according to design 1 and detection area of 3×3 mm².

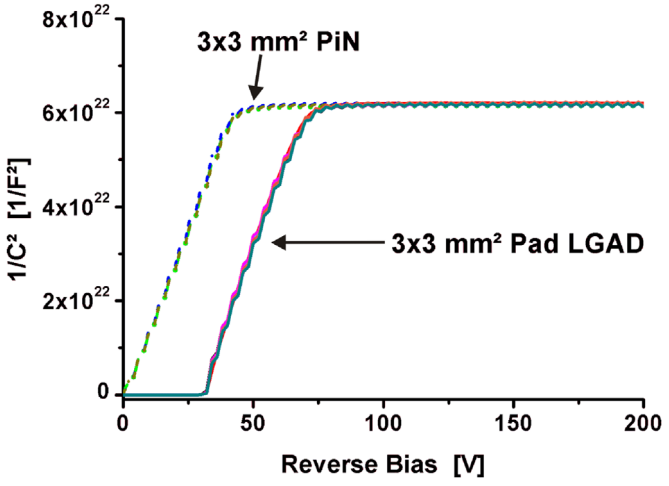

Fig. 2. $1/C^2$(V) curves of 300 μm pad LGAD and PiN detectors with edge termination according to designs 1, 2 and 3 and detection area of 3×3 mm².

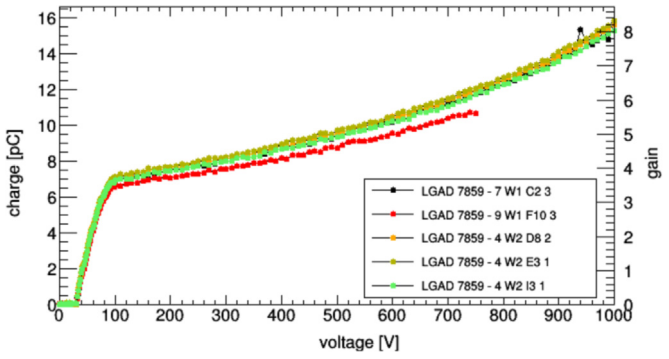

Fig. 3. Experimental collected charge from IR laser versus applied reverse voltage for different LGAD detectors with optimum P-well implantation dose.

when full depletion is reached at 150 V and reported in Fig. 4 (right hand side) is 1.4. The experimental evolution of the charge collection versus the reverse voltage in strip LGAD detectors is provided in Fig. 5, where a gain of 2 is obtained at 200 V when the laser illuminates the center of the strip.

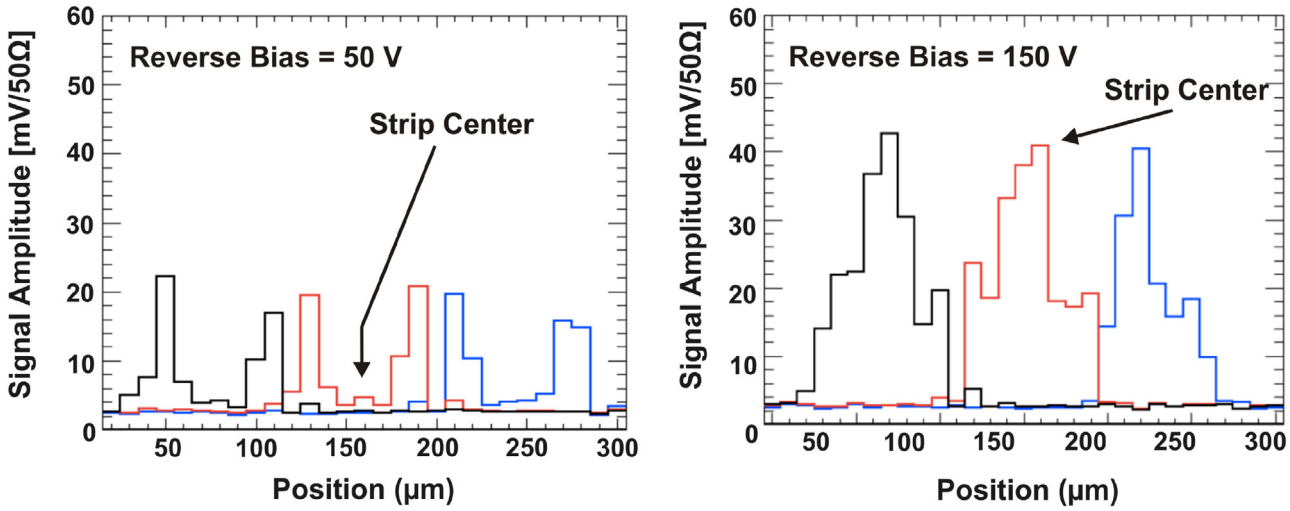

Fig. 4. Red laser scanning of three inner LGAD strips before full depletion (left) and after full depletion (right). The scanning step used for the measurements is 5 μm.

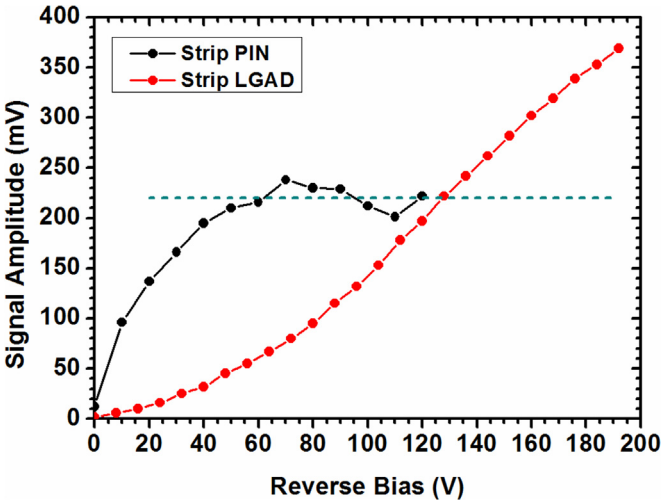

Fig. 5. Experimental results of charge collection measurements on strip LGAD and strip PiN detectors vs. the applied reverse voltage. The laser was illuminating the middle of the strip.

3. Inverse low gain avalanche detectors (iLGAD)

While strip LGAD detectors with low gain values were successfully fabricated, spatial non-uniformities due to the different multiplication from center to edge of each strip were also measured (see Fig. 4). The iLGAD strip cross section as drawn in Fig. 6 is designed to maximize the multiplication area while the segmentation is transferred to the p^+ ohmic side. A strip p-on-p detector [9] with internal gain is implemented where the collected signal is due to holes flowing back from multiplication junction. The consequence of such design leads to an increased detection time as compared with LGAD devices due to the lower mobility of holes. There are two possible ways to reduce the detection time: using thinner substrates with the inherent handling issue during wafer processing or implementing the iLGAD in the active silicon part of a Silicon-on-Insulator (SOI) wafer and then removing the handling substrate and the buried oxide.

TCAD simulations performed with the Sentaurus software [10] have shown that the voltage capability of the strip iLGAD is similar to that of the equivalent strip LGAD (>1000 V). However, the maximum electric field moves from the segmentation side, as it is the case in strip LGADs, to the multiplication side. A slight increase of the leakage current is observed in the strip iLGAD due to the higher multiplication area in comparison with the strip LGAD where the multiplication side is segmented. The electric field distribution at high reverse bias has been also simulated for both structures and it is plotted in Fig. 7. The strip LGAD structure exhibits a narrow high electric field region at the central part of each strip while the region of maximum electric field is uniformly distributed at the multiplication side in the case of the strip iLGAD.

The charge collection efficiency of the proposed iLGAD structure has been simulated by using minimum ionizing particles (MIP) and compared with the strip LGAD device. The simulation results clearly show (Fig. 8 left hand-side) a uniform gain wherever the MIP enters the structure for the iLGAD device which can

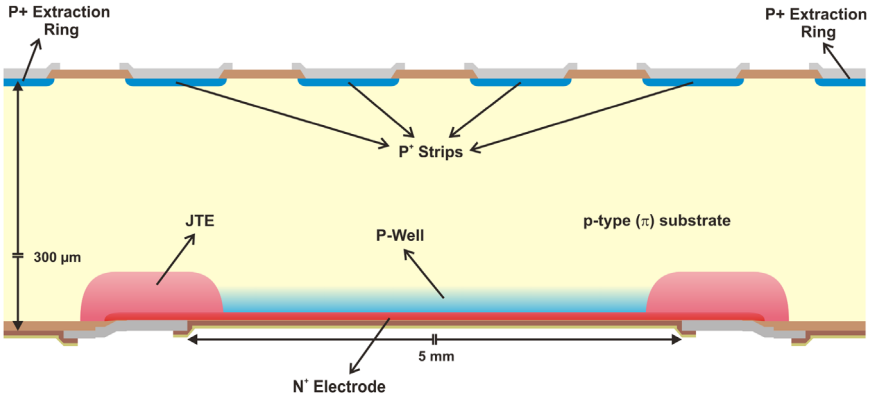

Fig. 6. Cross-section of the proposed strip iLGAD structure.

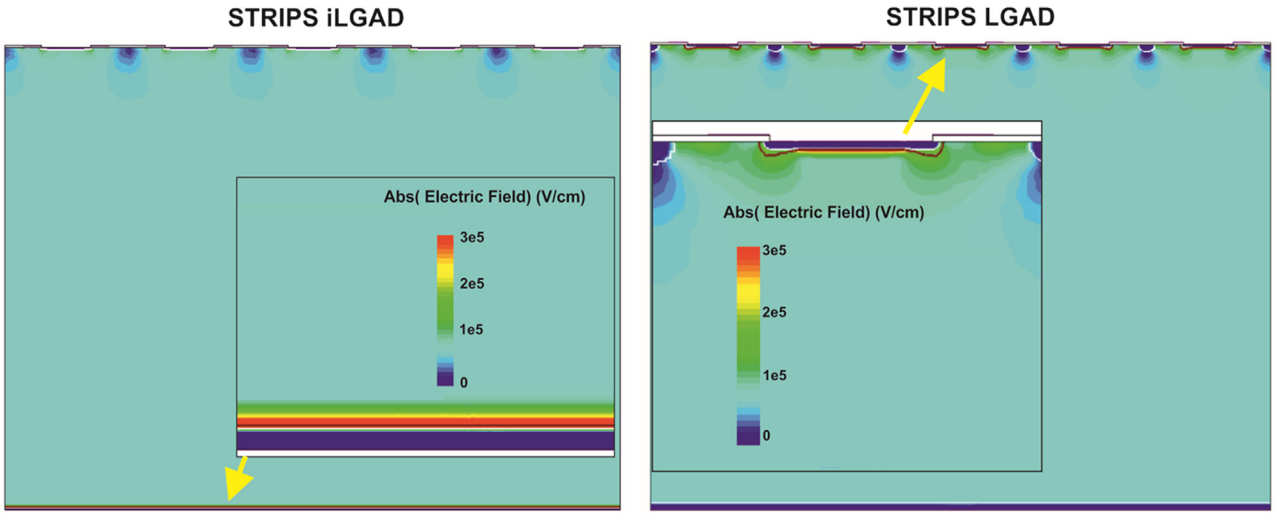

Fig. 7. Electric field distribution in the detection area of equivalent strip iLGAD (left) and strip LGAD (right). The arrows show the high electric field area in the two structures.

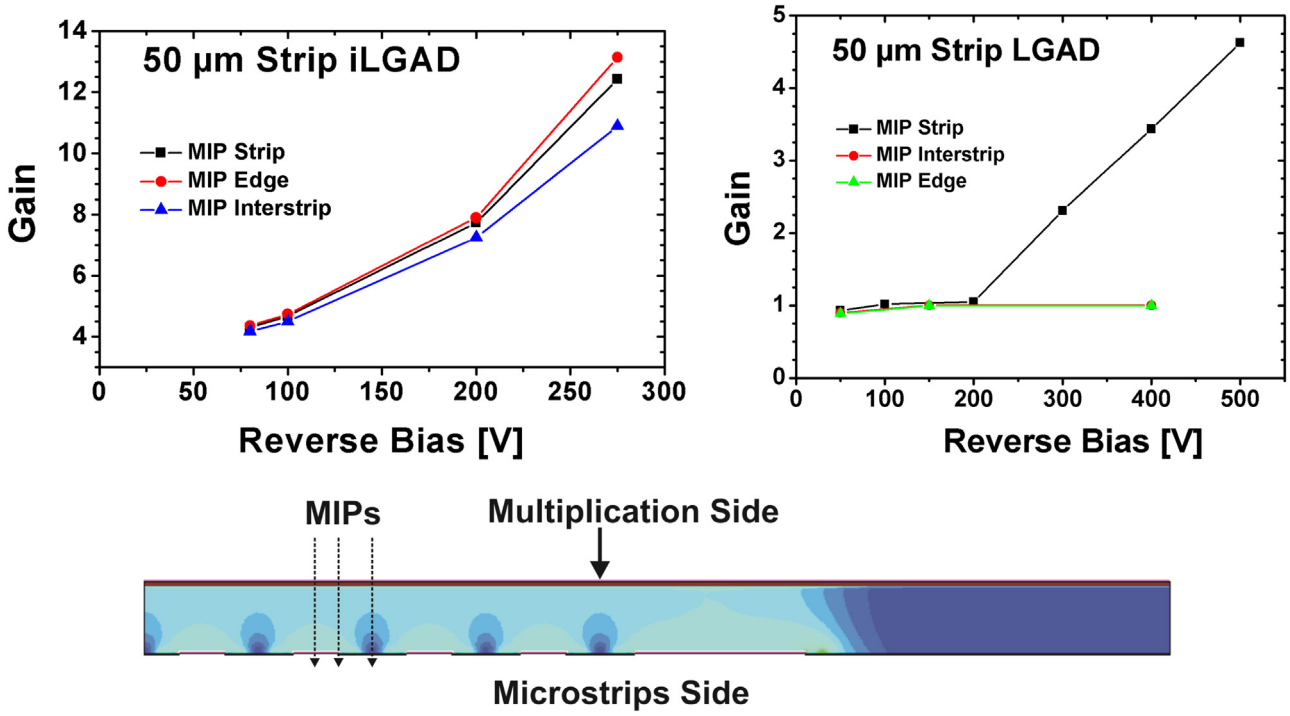

Fig. 8. Gain simulation by using MIP on strip iLGAD (left) and strip LGAD (right) structures. The position of the incident particles in the strip iLGAD is drawn at the bottom of the figure.

be explained by the non-segmented multiplication junction as with respect to LGAD devices. The iLGAD design is implemented with 50 μm silicon layer of a SOI substrate which is fully depleted at 70 V. The strip LGAD (Fig. 8 right hand-side) exhibits gain only in the central part of the strip. The latter is simulated on 285 μm thick substrates that become fully depleted at 180 V, where the multiplication starts to be relevant.

iLGAD production batches have been launched to allow real measurements to optimally identify the needed design parameters for gain uniformity and accurate detection performance. Strip iLGAD detectors are initially fabricated on conventional p-type silicon substrates and in a second step SOI substrates will be used to obtain thin detectors with fast timing detection capabilities [11].

4. Conclusions

The electrical performances of the fabricated strip LGAD detectors demonstrated a supply voltage range of up to 1000 V with leakage current of 20 nA/cm^2. The gain linearity was found satisfactory in an operating voltage range of 200–800 V for a gain range from 4–6. However, red laser scanning measurements revealed a non-uniform multiplication across the strips, basically due to technological constraints.

Based on TCAD simulations, the strip iLGAD structure can provide similar voltage capability and leakage current with the benefit of a uniform gain across the strips due to the non-segmentation of the multiplication junction.

Acknowledgments

This work was developed in the framework of the CERN RD50 collaboration and financed by the Spanish Ministry of Economy and Competitiveness through the Particle Physics National Program (FPA2013-48308-C2-2-P, FPA2014-55295-C3-2-R and FPA2013-48387-C6-1-P). This project has received funding from the European Union's Horizon 2020 Research and Innovation program under Grant Agreement no. 654168 (AIDA-2020).

References

[1] G. Lutz, Semiconductor Radiation Detectors, Device Physics, Springer editor.
[2] I. Tapan, et al., Avalanche photodiodes as proportional particle detectors, Nucl. Instrum. Methods Phys. Res. A 388 (1997) 79–90.
[3] G. Pellegrini, et al., Technology developments and first measurements of low gain avalanche detectors (LGAD) for high energy physics applications, Nucl. Instrum. Methods Phys. Res. A 765 (2014) 12–16.
[4] G. Kramberger, et al., Radiation Effects in Low Gain Avalanche Detectors After Hadron Irradiations, 2015, http://dx.doi.org/10.1088/1748-0221/10/07/P07006.
[5] G. Pellegrini, Recent developments on LGAD and iLGAD detectors for tracking and timing applications, Presented at the 10th International "Hiroshima" Symposium on the Development and Application of Semiconductor Tracking Detectors, Xi'an, China, September 2015, pp. 25–29.
[6] P. Fernández-Martínez, et al., Design and fabrication of an optimum peripheral region for low gain avalanche detectors, Nucl. Instrum. Methods Phys. Res. A 821 (2016) 93–100.
[7] V.A.K. Temple, Junction termination extension (JTE), A new technique for increasing avalanche breakdown voltage and controlling surface electric fields in P–N junctions. Electron Devices Meeting, 1977 International, vol. 23, http://dx.doi.org/10.1109/IEDM.1977.189277.
[8] S. Otero, Characterization of LGAD sensors from CNM Run 7859, 27th RD50 Workshop on Radiation Hard Semiconductor Devices for Very High Luminosity Colliders, CERN, Geneva, Switzerland, 2–4 December 2015.
[9] Lightstone et al., Avalanche Photodiode, United States Patent. Patent Number: 4654678. March 31, 1987.
[10] Technology Computer-Aided Design (TCAD), ⟨http://www.synopsys.com/⟩.
[11] H.F.-W. Sadrozinski, et al., Sensors for ultra-fast silicon detectors, Nucl. Instrum. Methods Phys. Res. A 765 (2014) 7–11.